Electronic Supplementary Material (ESI) for Journal of Materials Chemistry A.

Supplementary Information

A novel highly-stable two-dimensional boron phase with promising potentials in the energy fields

Yibo Zhang,[a] Mingyang Yang,[a] Ming Zhou,*[b] Shijia Feng,[a] Wenming Li [a] and Jiacong Lin [a]

[a]State Key Laboratory of Tribology, Department of Mechanical Engineering, Tsinghua University, Beijing 100084, People's Republic of China.

[b]Key Laboratory for Advanced Materials Processing Technology, Ministry of Education, Department of Mechanical Engineering, Tsinghua University, Beijing 100084, People's Republic of China.

*Corresponding author: zhouming@tsinghua.edu.cn

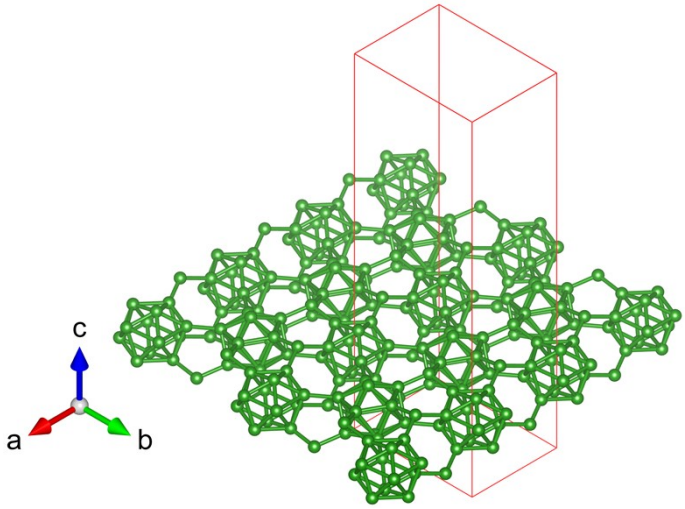

Fig. S1 Isometric view of the 3×2×1 supercell of the optimized structure of ε-B_{28}. The red frame contains a unit cell of ε-B_{28}. Some additional atoms are shown with regard to periodic boundary conditions.

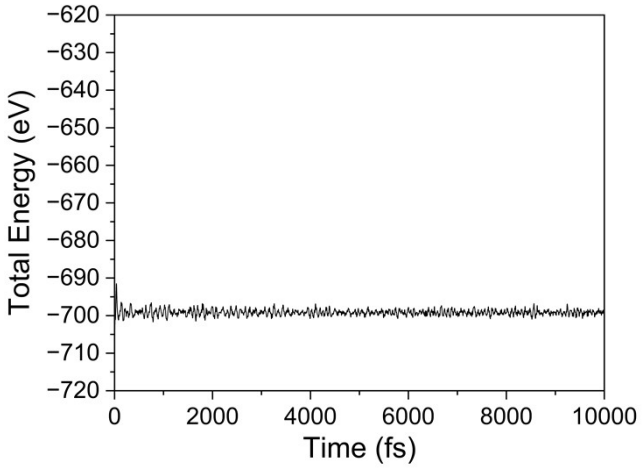

Fig. S2 AIMD energy fluctuations of a 2×2×1 ε-B_{28} supercell at 500 K during 10 ps time lapse. A single time step is set to 1 fs during the calculation.

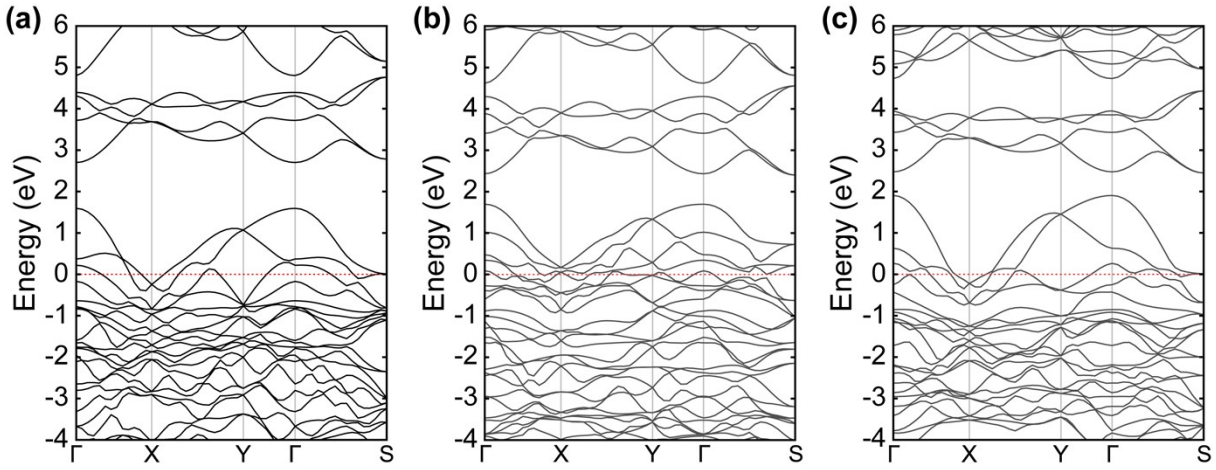

Fig. S3 HSE06 Band structures of ε-B_{28} with terminations. Band structures of (a) ε-$B_{28}F_4$, (b) ε-$B_{28}O_4$ and (c) ε-$B_{28}(OH)_4$. Fermi levels are set to zero.

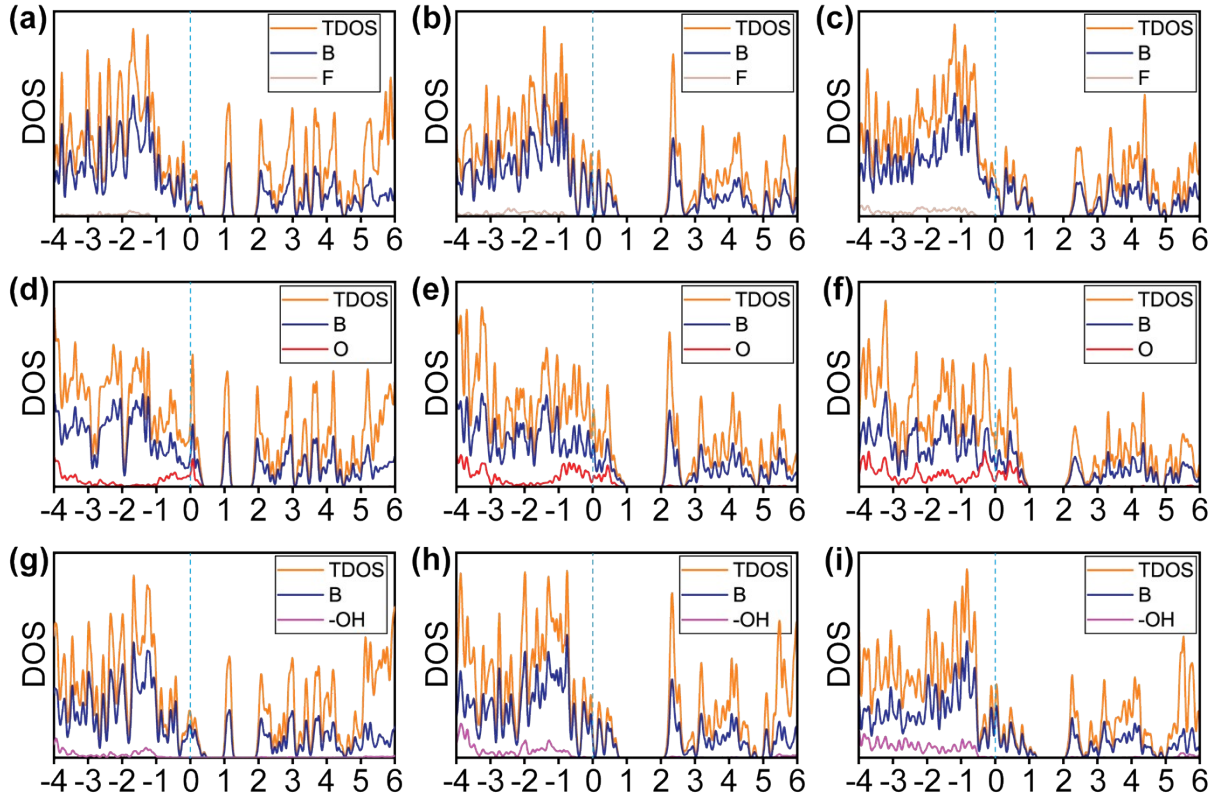

Fig. S4 Total and projected density of states of partially-functionalized ε-B_{28}. TDOS and PDOS of (a) ε-$B_{28}F$, (b) ε-$B_{28}F_2$, (c) ε-$B_{28}F_3$, (d) ε-$B_{28}O$, (e) ε-$B_{28}O_2$, (f) ε-$B_{28}O_3$, (g) ε-$B_{28}OH$, (h) ε-$B_{28}(OH)_2$ and (i) ε-$B_{28}(OH)_3$.

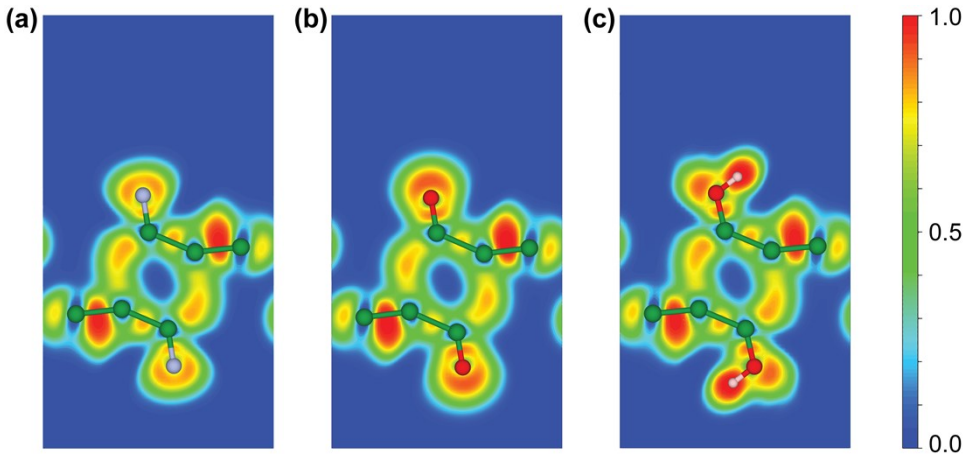

Figure S5. Electron localization function (ELF) of $\mathcal{E}$-B_{28} with terminations. ELF graphs of (200) sections of (a) $\mathcal{E}$-$B_{28}F_4$, (b) $\mathcal{E}$-$B_{28}O_4$ and (c) $\mathcal{E}$-$B_{28}(OH)_4$. ELF = 1.0 (red in color) corresponds to perfect localization and ELF = 0.5 (green in color) corresponds to the electron gas. The green, gray, red and pink balls represents the B, F, O and H atoms, respectively.

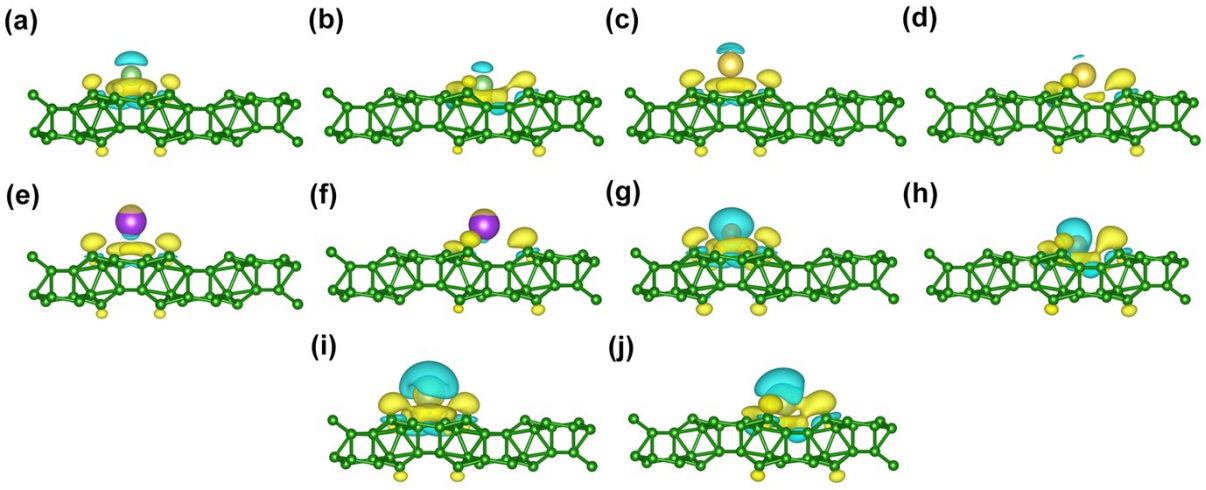

Fig. S6 Charge density difference of single metal atom adsorption on the surface of $\mathcal{E}$-B_{28}. Side views of charge density difference of Li adsorbed on (a) HEX site and (b) HEPT site, Na adsorbed on (c) HEX site and (d) HEPT site, K adsorbed on (e) HEX site and (f) HEPT site, Mg adsorbed on (g) HEX site and (h) HEPT site, and Ca adsorbed on (i) HEX site and (j) HEPT site. The isosurface level is set to 0.0025 e $Å^{-3}$. The yellow and blue regions depicts areas of charge accumulation and depletion, respectively.

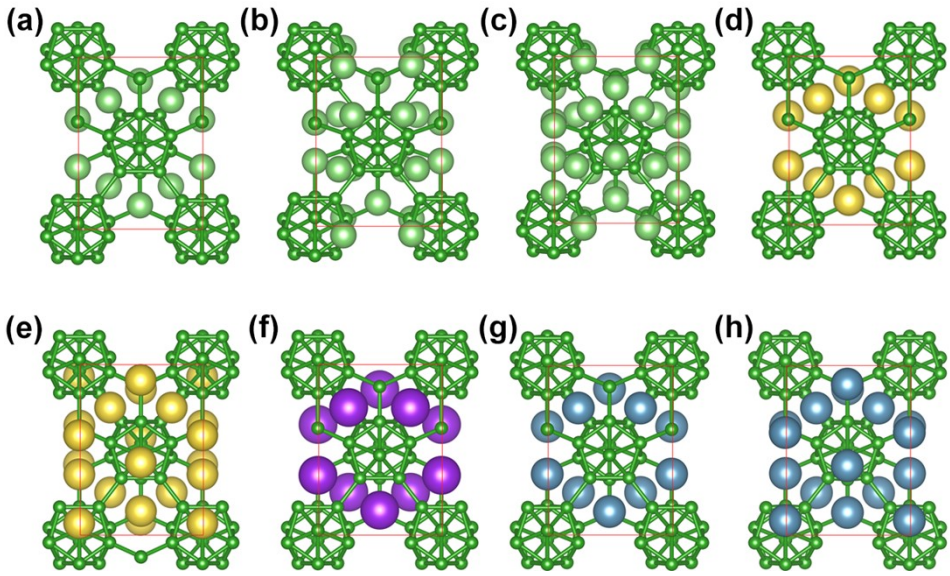

Fig. S7 Top views of single and double layer metal atoms adsorbed on $\mathcal{E}$-B_{28}. Stoichiometries of the presented configurations are (a) $B_{28}Li_8$, (b) $B_{28}Li_{16}$, (c) $B_{28}Li_{24}$, (d) $B_{28}Na_8$, (e) $B_{28}Na_{16}$, (f) $B_{28}K_8$, (g) $B_{28}Ca_8$, (h) $B_{28}Ca_{12}$. Red rectangles depict unit cells of the structures. Some additional atoms are shown with regard to periodic boundary conditions.

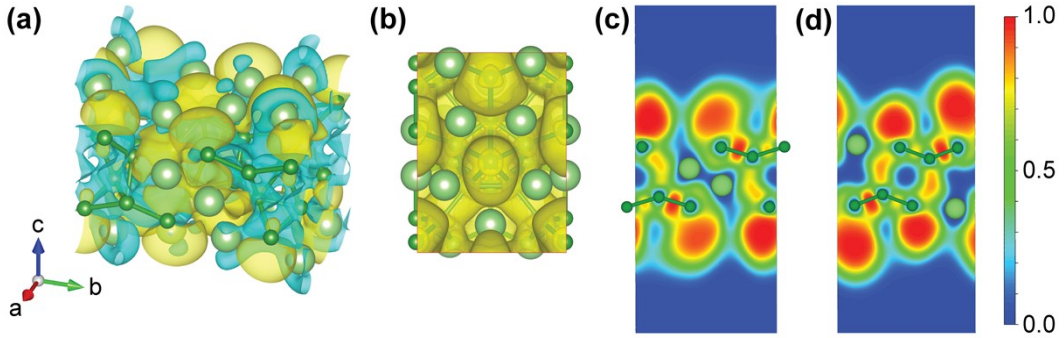

Fig. S8 Electronic structures of $B_{28}Li_{16}$. (a) Charge density difference of $B_{28}Li_{16}$. (b) Top view of the electron localization function of a single-cell $B_{28}Li_{16}$. ELF graphs of (c) (100) section, and (d) (200) section of $B_{28}Li_{16}$. The large and small green balls represent the Li and B atoms, respectively. ELF = 1.0 (red in color) corresponds to perfect localization and ELF = 0.5 (green in color) corresponds to the electron gas.

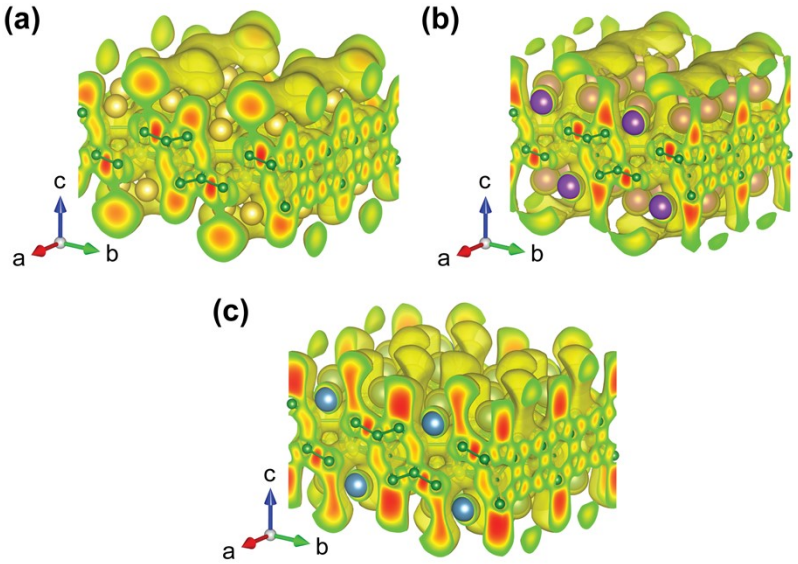

Fig. S9 3D views of electron localization function results of single layer metal atoms adsorption on the surface of $\mathcal{E}$-B_{28}. 2×2×1 supercells of three structures are shown for better understanding of the ELF profiles. Stoichiometries of the presented configurations are (a) $B_{28}Na_8$, (b) $B_{28}K_8$, and (c) $B_{28}Ca_8$. Yellow outlines depict the isosurfaces. On the sections, ELF = 1.0 (red in color) corresponds to perfect localization and ELF = 0.5 (green in color) corresponds to the electron gas.

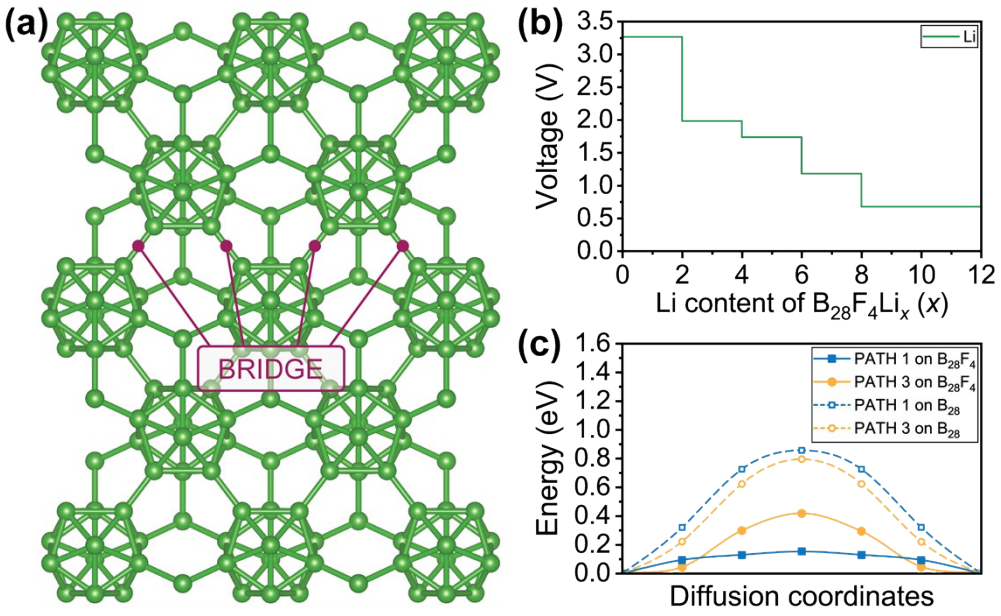

Fig. S10 Anode properties of functionalized $\mathcal{E}$-B_{28}. (a) Schematics of the additional BRIDGE site of Li on the surface of $\mathcal{E}$-$B_{28}O_4$. (b) OCV profile of Li atom adsorbed $\mathcal{E}$-B_{28} at different concentrations. (c) Diffusion behavior of Li atom on the surface of $\mathcal{E}$-$B_{28}F_4$ and pristine $\mathcal{E}$-B_{28}.

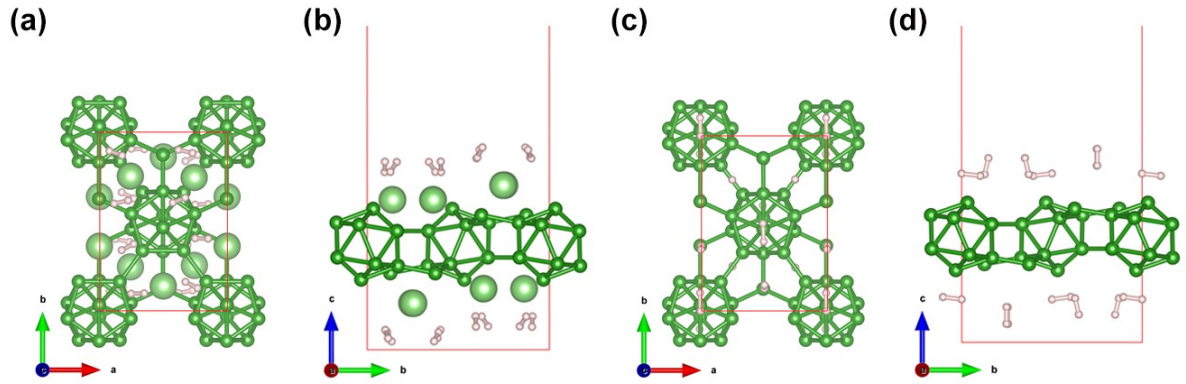

Fig. S11 Schematics of $\mathcal{E}$-B_{28} for hydrogen adsorption. (a) Top view and (b) side view of hydrogen molecules adsorbed on Li-decorated $\mathcal{E}$-B_{28} with stoichiometry of $B_{28}Li_8H_{32}$. (c) Top view and (d) side view of hydrogen molecules adsorbed on pristine $\mathcal{E}$-B_{28} with stoichiometry of $B_{28}H_{24}$. Red rectangles and lines mark unit cells of said structures.